JMM

The method based on quintic B-spline functions for addressing time-fractional advection-dispersion equations

Mohamed Adel[1], **Somaiyeh Abdi-mazraeh**[2], **Golamreza Zaki**[2], **Safar Irandoust-pakchin**[*2],

[1]*Department of Mathematics, Faculty of Science, Islamic University of Madinah, Medina, Saudia Arabia.*
[2]*Department of Applied Mathematics, Faculty of Mathematics, Statistics and Computer Sciences University of Tabriz, Tabriz, Iran*
Email(s): adel@sci.cu.edu.eg, s.abdi_m@tabrizu.ac.ir, zaki@tabrizu.ac.ir, s.irandoust@tabrizu.ac.ir

Abstract. This paper introduces a numerical method designed to address the fractional time advection-dispersion equation. Initially, the time dimension is discretized by employing the L1 method. Subsequently, quintic B-spline functions are utilized for the discretization of the spatial dimension. This approach yields a system of algebraic equations that can beefficiently solved. The proposed method is proven to be unconditionally stable. Numerical experiments provide compelling evidence of the method's efficiency and effectiveness.

1 Introduction

In recent decades, fractional differential equations (FDEs), with their unparalleled ability to model complex and nonlinear phenomena, have become a powerful tool in the hands of scientists and engineers. These equations, which generalize classical differential equations to non-integer orders, enable a more accurate and realistic description of many natural and artificial processes. From wave propagation in heterogeneous media to heat and mass transfer in complex materials, fractional equations play a key role in understanding and predicting the behavior of such systems [6–10, 15, 20].

Among the various types of FDEs, the fractional advection-dispersion equation (FADE) holds particular importance due to its wide range of applications in diverse fields. This equation, in general, describes the movement of particles or substances in a medium influenced by two main phenomena: advection and dispersion. Advection refers to the movement of particles due to the overall flow of the

medium, while dispersion refers to the movement of particles due to differences in concentration or other random factors. Employing fractional derivatives in this equation enables the modeling of more complex and non-standard behaviors. This equation, which combines the phenomena of advection and dispersion within the framework of fractional calculus, is widely used in modeling fluid flow in porous media, pollutant dispersion in the environment, and many other processes.

The FADEs can be classified into different types based on the nature of the fractional derivatives. Some of the most important types include:

- Time-fractional advection-dispersion equations (TFADEs): In these equations, the time derivatives are considered in a fractional form [2, 3, 5, 12, 14, 16, 18, 21, 29].

- Space-fractional advection-dispersion equations (*SFADEs*): In these equations, the spatial derivatives are considered in a fractional form [13, 25, 26].

- Time-space fractional advection-dispersion equations (*TSFADEs*): In these equations, both time and spatial derivatives are considered in a fractional form [17, 19, 28].

To solve the FADEs, researchers have employed a variety of numerical methods. For instance, Cao utilized the variable weights particle tracking method [5], while Singh applied the homotopy analysis method [29] and the homotopy perturbation method [28]. Saw et al. explored the use of the collocation method [26] and fourth-kind shifted Chebyshev polynomials [25]. Moghadam et al. implemented radial basis functions [17, 27], and Ravi Kanth et al. adopted the spline approximation method [21, 24, 31]. Additionally, Singh et al. applied the Jacobi collocation method [4, 30], and Bhardwaj et al. proposed an RBF-based meshless method [3]. However, given the complexity of these equations and the need for high accuracy, there remains a demand for more efficient and precise numerical methods.

This paper investigates the numerical solution of the following FADEs, with a particular emphasis on scenarios involving a variable time-fractional order:

$$
\begin{cases}
\frac{\partial^\alpha u(x,t)}{\partial t^\alpha} = \lambda \frac{\partial^2 u(x,t)}{\partial x^2} - \mu \frac{\partial u(x,t)}{\partial x} + f(x,t), & 0 \le t, \quad 0 \le x \le 1, \quad 0 < \alpha \le 1, \\
B.C.: \quad u(0,t) = 0, \quad u(1,t) = 0, \quad 0 \le t \le 1, \\
I.C.: \quad u(x,0) = g(x), \quad 0 \le x \le 1,
\end{cases}
\tag{1}
$$

where the term $f(x,t)$ is known as the source term, λ and μ represent the dispersion coefficient and the average fluid velocity, respectively. Moreover, the fractional derivative is in the Caputo sense

$$
\frac{\partial^\alpha u(x,t)}{\partial t^\alpha} =
\begin{cases}
\frac{1}{\Gamma(1-\alpha)} \int_0^t \frac{u_t(x,\tau)}{(t-\tau)^\alpha} d\tau, & 0 < \alpha < 1, \\
u_t(x,t), & \alpha = 1.
\end{cases}
\tag{2}
$$

The primary objective of this work is to develop and validate an effective and accurate numerical methodology for addressing problem (1). To facilitate this process, the L1 scheme is applied for the temporal discretization of the fractional derivative, while quintic B-spline (QB-S) functions are utilized for spatial discretization. In spectral methods, achieving higher approximation accuracy typically requires the inclusion of a larger number of terms. When orthogonal polynomials serve as basis functions, higher-degree polynomials are often required. In contrast, the proposed method employs splines with a maximum degree of five. The advantage of using quintic (degree five) splines over lower-degree alternatives, such as cubic splines, lies in their greater flexibility, which allows for more accurate representation

of complex solution behaviors without significantly increasing computational cost. The integration of these approaches transforms the FDE into a system of algebraic equations, thereby enhancing computational efficiency in obtaining solutions.

The organization of this paper is outlined as follows. In Section 2, essential definitions and notations related to QB-S functions are provided. In Section 3, a numerical method based on QB-S functions is presented, with its formulation and implementation being detailed. Subsequently, in Section 4, an analysis of the methods stability is conducted, and error estimates are derived to validate its accuracy. Finally, in Section 5, a series of numerical experiments are carried out to demonstrate the effectiveness and reliability of the proposed method.

2 Quintic B-spline functions

Spline functions are a type of mathematical function constructed from piecewise polynomials. These functions are defined by different polynomials over various intervals (pieces), and at the connection points (knots), smoothness conditions such as continuity and differentiability are maintained. Owing to their flexibility and capability to model complex data, spline functions are widely applied in mathematics, engineering, computer graphics, and data analysis.

The general characteristics of spline functions include the following:

- Piecewise nature: A spline function is defined by a polynomial in each specific interval.

- Knots: These are the points where the polynomials change. The knots can be uniformly or non-uniformly distributed.

- Smoothness: Spline functions are typically continuous and smooth up to a certain order of derivatives (e.g., first or second order) at the knots.

- Flexibility: Due to their piecewise structure, splines offer high flexibility in modeling data.

Formally, suppose that $M+1$ points $x_0 < x_1 < ... < x_M$ are given. The B-splines of degree 0 are denoted by $s_i^0(x)$ and defined as

$$s_i^0(x) = \begin{cases} 1, & x \in [x_i, x_{i+1}], \quad i \in \mathbb{Z}. \\ 0, & \text{otherwise.} \end{cases} \tag{3}$$

The functions $s_i^0(x)$ form the foundational basis for the recursive construction of all higher-degree B-splines. The fundamental recurrence relation that enables this construction is defined as follows:

$$s_i^k(x) = \frac{x - x_i}{x_{i+k} - x_i} s_i^{k-1}(x) + \frac{x_{i+k+1} - x}{x_{i+k+1} - x_{i+1}} s_{i+1}^{k-1}(x) \tag{4}$$
$$(k \geq 1).$$

Some important properties of B-splines functions are as follows:

- If $k \geq 1$ and $x \notin (x_i, x_{i+k+1})$ then $s_i^k(x) = 0$.

- Let $k \geq 0$. If $x \in (x_i, x_{i+k+1})$ then $s_i^k(x) > 0$.

Table 1: Values of QB-S functions and their derivatives at node points

	x_{i-3}	x_{i-2}	x_{i-1}	x_i	x_{i+1}	x_{i+2}	x_{i+3}
$s_i(x)$	0	$\frac{1}{120}$	$\frac{26}{120}$	$\frac{66}{120}$	$\frac{26}{120}$	$\frac{1}{120}$	0
$s_i'(x)$	0	$\frac{1}{24\Delta_x}$	$\frac{10}{24\Delta_x}$	0	$\frac{-10}{24\Delta_x}$	$\frac{-1}{24\Delta_x}$	0
$s_i''(x)$	0	$\frac{1}{6(\Delta_x)^2}$	$\frac{2}{6(\Delta_x)^2}$	$\frac{-6}{6(\Delta_x)^2}$	$\frac{2}{6(\Delta_x)^2}$	$\frac{1}{6(\Delta_x)^2}$	0
$s_i'''(x)$	0	$\frac{1}{2(\Delta_x)^3}$	$\frac{-2}{2(\Delta_x)^3}$	0	$\frac{2}{2(\Delta_x)^3}$	$\frac{-1}{2(\Delta_x)^3}$	0

- For all $k \geq 0$, $\sum_{i=-\infty}^{\infty} s_i^k(x) = 1$.

- For $k \geq 1$, the B-splines $s_i^k(x)$ belong to continuity class $C^{k-1}(\mathbb{R})$.

- For $k \geq 2$, $\frac{d}{dx} s_i^k(x) = \frac{k}{x_{i+k}-t_i} s_i^{k-1}(x) - \frac{k}{x_{i+k+1}-t_{i+1}} s_{i+1}^{k-1}(x)$.

- When $k = 1$, the equation is true for all x except $x = x_i, x_{i+1}, x_{i+2}$.

This study exclusively focuses on QB-S functions, corresponding to the scenario in which $k = 5$. For clarity and notational efficiency in subsequent analysis, the superscript '5' in the representation $s_i^5(x)$ will be omitted. Accordingly, these functions will henceforth be referred to simply as $s_i(x)$. The QB-S functions can be obtained from equations (3) and (4) as follow [22,23]:

$$
s_i(x) = \frac{(\Delta_x)^{-5}}{120}
\begin{cases}
(x-x_{i-3})^5, & x \in [x_{i-3}, x_{i-2}], \\
(x-x_{i-3})^5 - 6(x-x_{i-2})^5, & x \in [x_{i-2}, x_{i-1}], \\
(x-x_{i-3})^5 - 6(x-x_{i-2})^5 + 15(x-x_{i-1})^5, & x \in [x_{i-1}, x_i], \\
(x_{i+3}-x)^5 - 6(x_{i+2}-x)^5 + 15(x_{i+1}-x)^5, & x \in [x_i, x_{i+1}], \\
(x_{i+3}-x)^5 - 6(x_{i+2}-x)^5, & x \in [x_{i+1}, x_{i+2}], \\
(x_{i+3}-x)^5, & x \in [x_{i+2}, x_{i+3}], \\
0, & \text{otherwise.}
\end{cases}
\tag{5}
$$

It is easy to conclude that

$$
\sum_{k=-2}^{M+2} |s_k(x)| \leq \frac{93}{60}, \quad 0 \leq x \leq 1.
\tag{6}
$$

Furthermore, by substituting x_k for $k \in \{i-3, i-2, i-1, i, i+1, i+2, i+3\}$ instead of x in $s_i(x)$, one can easily derive the results delineated in the Table 1.

Assuming $u(x, t_j) = u^j(x)$, the approximation function of $u^j(x)$ can be obtained as follows:

$$
\tilde{u}^j(x) = \sum_{k=-2}^{M+2} c_k^j s_k(x).
\tag{7}
$$

Moreover, it can be resulted that

$$\tilde{u}^j(x_i) = \frac{1}{120}(c_{i-2}^j + 26c_{i-1}^j + 66c_i^j + 26c_{i+1}^j + c_{i+2}^j),$$

$$\tilde{u}_x^j(x_i) = \frac{1}{24(\Delta_x)}(-c_{i-2}^j - 10c_{i-1}^j + 10c_{i+1}^j + c_{i+2}^j),$$

$$\tilde{u}_{xx}^j(x_i) = \frac{1}{6(\Delta_x)^2}(c_{i-2}^j + 2c_{i-1}^j - 6c_i^j + 2c_{i+1}^j + c_{i+2}^j),$$

$$\tilde{u}_{xxx}^j(x_i) = \frac{1}{2(\Delta_x)^3}(-c_{i-2}^j + 2c_{i-1}^j - 2c_{i+1}^j + c_{i+2}^j). \tag{8}$$

To establish the support for quintic B-spline functions, the initial partition $0 = x_0 < x_1 < x_2 < ... < x_M = 1$ is extended by introducing ten additional grid points. These extra points are positioned outside the primary domain, specifically at $x_{-5} < x_{-4} < x_{-3} < x_{-2} < x_{-1}$ on the left and $x_{M+1} < x_{M+2} < x_{M+3} < x_{M+4} < x_{M+5}$ on the right. The set of QB-S functions is then defined as

$$\bar{S}_5 = \{s_{-2}(x), s_{-1}(x), s_{-0}(x), ..., s_{M+1}(x), s_{M+2}(x)\}.$$

The space spanned by these functions is denoted as $S^* = \text{span}\bar{S}$. Now, let $\hat{u}^j(x)$ be an interpolation function to $u^j(x)$, defined as

$$\hat{u}^j(x) = \sum_{k=-2}^{M+2} \hat{c}_k^j s_k(x). \tag{9}$$

Therefore, it is clear that $\hat{u}^j(x)$ satisfies the following interpolating conditions:

$$\hat{u}^j(x_i) = u^j(x_i) \quad i = 0, 1, ..., M.$$

Theorem 1. *([23]) Let $\hat{u}^j(x)$ be the quintic spline interpolant of $u^j(x) \in C^{10}[0,1]$, then the following relations hold at the grid points x_i for $i = 0, 1, ..., M,$:*

$$\hat{u}_x^j(x_i) = u_x^j(x_i) + O(\Delta_x^6),$$

$$\hat{u}_{xx}^j(x_i) = u_{xx}^j(x_i) + \frac{(\Delta_x^4)}{720}u_{xxxxxx}^j(x_i) + O(\Delta_x^6),$$

$$\hat{u}_{xxx}^j(x_i) = u_{xxx}^j(x_i) - \frac{(\Delta_x^4)}{240}u_{xxxxxxx}^j(x_i) + O(\Delta_x^6),$$

$$\hat{u}_{xxxx}^j(x_i) = u_{xxxx}^j(x_i) - \frac{(\Delta_x^2)}{12}u_{xxxxxx}^j(x_i) + \frac{(\Delta_x^4)}{240}u_{xxxxxxxx}^j(x_i) + O(\Delta_x^6). \tag{10}$$

Theorem 2. *([11]) Let $\hat{u}^j(x)$ be a unique quintic spline interpolant to the exact solution $u^j(x) \in C^{10}[0,1]$, then we have*

$$\|\frac{\partial^k}{\partial x^k}(\hat{u}^j(x) - u^j(x))\|_\infty \le R\Delta_x^{6-k}, \quad k = 0, 1, 2, 3, 4, \tag{11}$$

where the constant R is independent of Δ_x.

3   Derivation of the method

In this section, we develop a higher-order numerical method to approximate the solution of the TFADE (1). To facilitate the discretization process, assume that

$$\begin{cases} x_i = i\Delta_x, \ \ \Delta_x = 1/M, \ \ i = 0, 1, ..., M, \\ t_j = j\Delta_t, \ \ \Delta_t = 1/N, \ \ j = 0, 1, ..., N. \end{cases} \tag{12}$$

By employing the L1 method, the fractional partial derivative of $u(x,t)$ with respect to the variable t can be discretized as follows:

$$\begin{aligned}
\frac{\partial^\alpha u(x,t_j)}{\partial t^\alpha} &= \frac{1}{\Gamma(1-\alpha)} \int_0^{t_j} \frac{u_\tau(x,\tau)}{(t_j-\tau)^\alpha} d\tau \\
&= \frac{1}{\Gamma(1-\alpha)} \sum_{k=0}^{j-1} \int_{k\Delta_x}^{(k+1)\Delta_x} \frac{u_\tau(x,\tau)}{(t_j-\tau)^\alpha} d\tau \\
&= \frac{1}{\Gamma(1-\alpha)} \sum_{k=0}^{j-1} \frac{u(x,t_{k+1}) - u(x,t_k)}{\Delta_t} \int_{k\Delta_x}^{(k+1)\Delta_x} (t_j-\tau)^{-\alpha} d\tau + T_{\Delta_t}^j \\
&= \frac{(\Delta_t)^{-\alpha}}{\Gamma(2-\alpha)} \sum_{k=0}^{j-1} ((j-k)^{1-\alpha} - (j-k-1)^{1-\alpha})(u(x,t_{k+1}) - u(x,t_k)) \\
&\quad + T_{\Delta_t}^j \\
&= \sum_{k=0}^{j-1} b_k^j (u(x,t_{k+1}) - u(x,t_k)) + T_{\Delta_t}^j \\
&= -b_0^j u(x,t_0) + \sum_{k=1}^{j-1} (b_{k-1}^j - b_k^j) u(x,t_k) + b_{j-1}^j u(x,t_j) + T_{\Delta_t}^j,
\end{aligned} \tag{13}$$

where

$$\begin{aligned}
\sigma &= \frac{(\Delta_t)^{-\alpha}}{\Gamma(2-\alpha)}, \ \ T_{\Delta_t}^j \le C_u \Delta_t^{2-\alpha}, \\
b_k^j &= \sigma((j-k)^{1-\alpha} - (j-k-1)^{1-\alpha}), \ \ k = 0, 1, ..., j-1,
\end{aligned} \tag{14}$$

and C_u is a constant depending on u.

Using Eq. (7), Eq. (13) can be briefly written as

$$\begin{aligned}
\frac{\partial^\alpha u(x,t_j)}{\partial t^\alpha} &= \sum_{k=0}^{j} d_k^j u(x,t_k) + T_{\Delta_t}^j \\
&\cong \sum_{k=0}^{j} d_k^j \tilde{u}^k(x) \\
&= \sum_{k=0}^{j} d_k^j \sum_{l=-2}^{M+2} c_l^k s_l(x),
\end{aligned} \tag{15}$$

where

$$d_0^j = -b_0^j, \quad d_j^j = b_{j-1}^j = \sigma, \quad d_k^j = b_{k-1}^j - b_k^j, \quad k = 1, 2, ..., j-1. \tag{16}$$

Furthermore $\sum_{k=0}^j d_k^j = 0$ and $\sum_{k=0}^{j-1} d_k^j = \sigma$.

On the other hand, for space discretization, one can write

$$\lambda \tilde{u}_{xx}^j(x) - \mu \tilde{u}_x^j(x) = \sum_{l=-2}^{M+2} (c_l^j (\lambda s_l''(x) - \mu s_l'(x)). \tag{17}$$

Replacing (15) and (17) in (1) gives

$$\sum_{k=0}^j d_k^j \sum_{l=-2}^{M+2} c_l^k s_l(x) = \sum_{l=-2}^{M+2} c_l^j (\lambda s_l''(x) - \mu s_l'(x)) + f^j(x). \tag{18}$$

According to the collocation technique, it can be resulted that

$$\sum_{k=0}^j d_k^j \sum_{l=-2}^{M+2} c_l^k s_l(x_i) = \sum_{l=-2}^{M+2} c_l^j (\lambda s_l''(x_i) - \mu s_l'(x_i)) + f^j(x_i). \tag{19}$$

Now, by using Table 1, it can be derived that

$$\sum_{k=0}^j d_k^j (c_{i-2}^k \frac{1}{120} + c_{i-1}^k \frac{26}{120} + c_i^k \frac{66}{120} + c_{i+1}^k \frac{26}{120} + c_{i+2}^k \frac{1}{120})$$
$$= c_{i-2}^j (\frac{\lambda}{6(\Delta_x)^2} - \frac{-\mu}{24\Delta_x}) + c_{i-1}^j (\frac{2\lambda}{6(\Delta_x)^2} - \frac{-10\mu}{24\Delta_x}) + c_i^j (\frac{-6\lambda}{6(\Delta_x)^2})$$
$$+ c_{i+1}^j (\frac{2\lambda}{6(\Delta_x)^2} - \frac{10\mu}{24\Delta_x}) + c_{i+2}^j (\frac{\lambda}{6(\Delta_x)^2} - \frac{\mu}{24\Delta_x}) + f_i^j. \tag{20}$$

Assuming $\zeta_0 = \frac{1}{120}$, $\zeta_1 = \frac{1}{24\Delta_x}$, $\zeta_2 = \frac{1}{6(\Delta_x)^2}$, $\zeta_3 = \frac{1}{2(\Delta_x)^3}$, $d_j^j = \sigma$, one can write (20) as

$$c_{i-2}^j (\lambda \zeta_2 + \mu \zeta_1 - \sigma \zeta_0) + c_{i-1}^j (2\lambda \zeta_2 + 10\mu \zeta_1 - 26\sigma \zeta_0) + c_i^j (-6\lambda \zeta_2 - 66\sigma \zeta_0)$$
$$+ c_{i+1}^j (2\lambda \zeta_2 - 10\mu \zeta_1 - 26\sigma \zeta_0) + c_{i+2}^j (\lambda \zeta_2 - \mu \zeta_1 - \sigma \zeta_0)$$
$$= \zeta_0 \sum_{k=0}^{j-1} d_k^j (c_{i-2}^k + 26c_{i-1}^k + 66c_{i-2}^k + 26c_{i-2}^k + c_{i-2}^k) - f_i^j. \tag{21}$$

To put it briefly, it can be said that

$$a_1 c_{i-2}^j + a_2 c_{i-1}^j + a_3 c_i^j + a_4 c_{i+1}^j + a_5 c_{i+2}^j$$
$$= \zeta_0 \sum_{k=0}^{j-1} d_k^j (c_{i-2}^k + 26c_{i-1}^k + 66c_i^k + 26c_{i+1}^k + c_{i+2}^k) - f_i^j, \tag{22}$$

where

$$a_1 = (\lambda \zeta_2 + \mu \zeta_1 - \sigma \zeta_0),$$

$$a_2 = (2\lambda\zeta_2 + 10\mu\zeta_1 - 26\sigma\zeta_0),$$
$$a_3 = (-6\lambda\zeta_2 - 66\sigma\zeta_0),$$
$$a_4 = (2\lambda\zeta_2 - 10\mu\zeta_1 - 26\sigma\zeta_0),$$
$$a_5 = (\lambda\zeta_2 - \mu\zeta_1 - \sigma\zeta_0).$$

Considering the boundary conditions, one con derive that

$$c_{-2}^j + 26c_{-1}^j + 66c_0^j + 26c_1^j + c_2^j = 0, \tag{23}$$

$$c_{M-2}^j + 26c_{M-1}^j + 66c_M^j + 26c_{M+1}^j + c_{M+2}^j = 0. \tag{24}$$

From Eqs. (22) for $0 \le i \le M$ and (23)-(24) a linear system of $M+3$ equations in $M+5$ unknowns is obtained. To solve this system uniquely, two auxiliary equations are needed. For this purpose, by taking the derivative of relation (18) with respect to the variable x, it can be written that

$$\sum_{k=0}^{j} d_k^j \sum_{l=-2}^{M+2} c_l^k s_l'(x) = \sum_{l=-2}^{M+2} c_l^j (\lambda s_l'''(x) - \mu s_l''(x)) + f'^j(x). \tag{25}$$

Furthermore, for $i = 0$, it can be resulted that

$$\zeta_1 \sum_{k=0}^{j-1} d_k^j (-c_{-2}^k - 10c_{-1}^k + 10c_1^k + c_2^k)$$
$$= c_{-2}^j(-\lambda\zeta_3 - \mu\zeta_2 + \sigma\zeta_1) + c_{-1}^j(2\lambda\zeta_3 - 2\mu\zeta_2 + 10\sigma\zeta_1) + c_0^j(6\mu\zeta_2) \tag{26}$$
$$+ c_1^j(-2\lambda\zeta_3 - 2\mu\zeta_2 - 10\sigma\zeta_1) + c_2^j(1\lambda\zeta_3 - \mu\zeta_2 - \sigma\zeta_1) + f'^j(0),$$

and for $i = M$, it can be shown that

$$\zeta_1 \sum_{k=0}^{j-1} d_k^j (-c_{M-2}^k - 10c_{M-1}^k + 10c_{M+1}^k + c_{M+2}^k)$$
$$= c_{M-2}^j(-\lambda\zeta_3 - \mu\zeta_2 + \sigma\zeta_1) + c_{M-1}^j(2\lambda\zeta_3 - 2\mu\zeta_2 + 10\sigma\zeta_1) + c_M^j(6\mu\zeta_2) \tag{27}$$
$$+ c_{M+1}^j(-2\lambda\zeta_3 - 2\mu\zeta_2 - 10\sigma\zeta_1) + c_{M+2}^j(1\lambda\zeta_3 - \mu\zeta_2 + \sigma\zeta_1) + f'^j(1).$$

Assuming that

$$\hat{a}_1 = (-\lambda\zeta_3 - \mu\zeta_2 + \sigma\zeta_1),$$
$$\hat{a}_2 = (2\lambda\zeta_3 - 2\mu\zeta_2 + 10\sigma\zeta_1),$$
$$\hat{a}_3 = (0\lambda\zeta_3 + 6\mu\zeta_2 - 0\sigma\zeta_1),$$
$$\hat{a}_4 = (-2\lambda\zeta_3 - 2\mu\zeta_2 - 10\sigma\zeta_1),$$
$$\hat{a}_5 = (1\lambda\zeta_3 - \mu\zeta_2 - \sigma\zeta_1),$$

Eqs. (26)-(27) can be written as

$$\hat{a}_1 c_{-2}^j + \hat{a}_2 c_{-1}^j + \hat{a}_3 c_0^j + \hat{a}_4 c_1^j + \hat{a}_5 c_2^j$$

$$= \zeta_1 \sum_{k=0}^{j-1} d_k^j(-c_{-2}^k - 10c_{-1}^k + 10c_1^k + c_2^k) - f'^j(0), \tag{28}$$

$$\hat{a}_1 c_{M-2}^j + \hat{a}_2 c_{M-1}^j + \hat{a}_3 c_M^j + \hat{a}_4 c_{M+1}^j + \hat{a}_5 c_{M+2}^j$$

$$= \zeta_1 \sum_{k=0}^{j-1} d_k^j(-c_{M-2}^k - 10c_{M-1}^k + 10c_{M+1}^k + c_{M+2}^k) - f'^j(1). \tag{29}$$

From Eqs. (22) for $0 \le i \le M$, and (23)-(24) as well as (28)-(29) a linear system of $M+5$ equations with $M+5$ unknowns $c_{-2}^j, c_{-1}^j, ..., c_{M+1}^j, c_{M+2}^j$ is obtained. In the matrix form this system can be written as

$$AC^j = \zeta_0(d_{j-1}^j BC^{j-1} + d_{j-2}^j BC^{j-2} + ... + d_0^j BC^0) - F^j$$
$$= \zeta_0 B(d_{j-1}^j C^{j-1} + d_{j-2}^j C^{j-2} + ... + d_0^j C^0) - F^j, \tag{30}$$

or

$$C^j = A^{-1}(\zeta_0 B \sum_{k=0}^{j-1} d_k^j C^k - F^j), \tag{31}$$

where

$$C^j = [c_{-2}^j, c_{-1}^j, c_0^j, ..., c_M^j, c_{M+1}^j, c_{M+2}^j]^T,$$
$$F^j = [f(x_{-2}, t_j), f(x_{-1}, t_j), f(x_0, t_j), ..., f(x_M, t_j), f(x_{M+1}, t_j), f(x_{M+2}, t_j)]^T,$$

as well as A,B are the quasi five-diagonal $(M+5) \times (M+5)$ matrices as follows:

$$A = \begin{bmatrix} 1 & 26 & 66 & 26 & 1 & 0 & \cdots & 0 \\ \hat{a}_1 & \hat{a}_2 & \hat{a}_3 & \hat{a}_4 & \hat{a}_5 & 0 & \cdots & 0 \\ a_1 & a_2 & a_3 & a_4 & a_5 & 0 & \cdots & 0 \\ 0 & a_1 & a_2 & a_3 & a_4 & a_5 & \cdots & 0 \\ \vdots & \vdots & \vdots & \vdots & \vdots & \ddots & \ddots & \vdots \\ 0 & \cdots & a_1 & a_2 & a_3 & a_4 & a_5 & 0 \\ 0 & \cdots & 0 & a_1 & a_2 & a_3 & a_4 & a_5 \\ 0 & \cdots & 0 & \hat{a}_1 & \hat{a}_2 & \hat{a}_3 & \hat{a}_4 & \hat{a}_5 \\ 0 & \cdots & 0 & 1 & 26 & 66 & 26 & 1 \end{bmatrix},$$

$$B = \begin{bmatrix} 0 & 0 & 0 & 0 & 0 & 0 & \cdots & 0 \\ -\zeta_1/\zeta_0 & -10\zeta_1/\zeta_0 & 0 & 10\zeta_1/\zeta_0 & \zeta_1/\zeta_0 & 0 & \cdots & 0 \\ 1 & 26 & 66 & 26 & 1 & 0 & \cdots & 0 \\ 0 & 1 & 26 & 66 & 26 & 1 & \cdots & 0 \\ \vdots & \vdots & \vdots & \vdots & \vdots & \ddots & \ddots & \vdots \\ 0 & \cdots & 1 & 26 & 66 & 26 & 1 & 0 \\ 0 & \cdots & 0 & 1 & 26 & 66 & 26 & 1 \\ 0 & \cdots & 0 & -\zeta_1/\zeta_0 & -10\zeta_1/\zeta_0 & 0 & 10\zeta_1/\zeta_0 & \zeta_1/\zeta_0 \\ 0 & \cdots & 0 & 0 & 0 & 0 & 0 & 0 \end{bmatrix}.$$

It is worth mentioning that to obtain the $C^0 = [c^0_{-2}, c^0_{-1}, c^0_0, ..., c^0_M, c^0_{M+1}, c^0_{M+2}]^T$, the initial condition $g(x) = \sum_{k=-2}^{M+2} c^0_k s_k(x)$ is used, and the following relation is derived:

$$C^0 = A_0^{-1} G_0,\tag{32}$$

where

$$A_0 = \begin{bmatrix} -1 & -10 & 0 & 10 & 1 & 0 & \cdots & 0 \\ 1 & 2 & -6 & 2 & 1 & 0 & \cdots & 0 \\ 1 & 26 & 66 & 26 & 1 & 0 & \cdots & 0 \\ 0 & 1 & 26 & 66 & 26 & 1 & \cdots & 0 \\ \vdots & \vdots & \vdots & \vdots & \vdots & \ddots & \ddots & \vdots \\ 0 & \cdots & 1 & 26 & 66 & 26 & 1 & 0 \\ 0 & \cdots & 0 & 1 & 26 & 66 & 26 & 1 \\ 0 & \cdots & 0 & 1 & 2 & -6 & 2 & 1 \\ 0 & \cdots & 0 & -1 & -10 & 0 & 10 & 1 \end{bmatrix}$$

and

$$G^0 = [\zeta_2 g''(x_0), \zeta_1 g'(x_0), \zeta_0 g(x_0), ..., \zeta_0 g(x_M), \zeta_1 g'(x_0), \zeta_2 g''(x_M)]^T.$$

4 Stability and convergence analysis

The primary objective of this section is to analyze the convergence and stability of the proposed method. Let $u(x_i, t_j)$ and $\tilde{u}(x_i, t_j)$ be the exact solution and approximate solution for problem (1), respectively.

Theorem 3. *The proposed numerical scheme defined as* (31) *for solving the FADE* (1) *is unconditionally stable.*

Proof. The Neumann-Fourier method is used to analyze the stability of the proposed method (31). For this purpose, suppose that $f(x,t) = 0$ and

$$\varepsilon_i^j = u(x_i, t_j) - \tilde{u}(x_i, t_j).\tag{33}$$

By using Eq. (33), the error equation can be obtained as

$$a_1 \varepsilon_{i-2}^j + a_2 \varepsilon_{i-1}^j + a_3 \varepsilon_i^j + a_4 \varepsilon i + 1^j + a_5 \varepsilon_{i+2}^j$$
$$= \zeta_0 \sum_{k=0}^{j-1} d_k^j (\varepsilon_{i-2}^k + 26\varepsilon_{i-1}^k + 66\varepsilon_i^k + 26\varepsilon_{i+1}^k + \varepsilon_{i+2}^k).\tag{34}$$

The error function ε_i^j can be chosen in a Fourier form as

$$\varepsilon_i^j = \Phi^j e^{\mathrm{i} i \theta},\tag{35}$$

where $\theta = \Delta_x \Delta_t$, $\mathrm{i} = \sqrt{-1}$, and Φ is the time dependent parameter of error and the exponential term represents the spatial dependence. Substituting Eq. (35) into Eq. (34), one can derive that

$$\Phi^j e^{\mathrm{i} i \theta} [a_1 e^{\mathrm{i}(-2)\theta} + a_2 e^{\mathrm{i}(-1)\theta} + a_3 + a_4 e^{\mathrm{i}(1)\theta} + a_5 e^{\mathrm{i}(2)\theta}]$$

$$= e^{\mathrm{i}i\theta}[\zeta_0 \sum_{k=0}^{j-1} d_k^j \Phi^k (e^{\mathrm{i}(-2)\theta} + 26e^{\mathrm{i}(-1)\theta} + 66e^{\mathrm{i}(0)\theta} + 26e^{\mathrm{i}(1)\theta} + e^{\mathrm{i}(2)\theta})]. \tag{36}$$

The above equation can be rewritten as

$$\Phi^j[(\lambda \zeta_2 + \mu \zeta_1 - \sigma \zeta_0)e^{\mathrm{i}(-2)\theta} + (2\lambda \zeta_2 + 10\mu \zeta_1 - 26\sigma \zeta_0)e^{\mathrm{i}(-1)\theta}$$
$$+(-6\lambda \zeta_2 - 66\sigma \zeta_0) + (2\lambda \zeta_2 - 10\mu \zeta_1 - 26\sigma \zeta_0)e^{\mathrm{i}(1)\theta} + (\lambda \zeta_2 - \mu \zeta_1 - \sigma \zeta_0)e^{\mathrm{i}(2)\theta}]$$
$$= \zeta_0 \sum_{k=0}^{j-1} d_k^j \Phi^k (2cos(2\theta) + 52cos(\theta) + 66),$$

$$\Rightarrow \Phi^j[(2\lambda \zeta_2 - 2\sigma \zeta_0)cos(2\theta) + (4\lambda \zeta_2 - 52\sigma \zeta_0)cos(\theta) - 2\mathrm{i}\mu \zeta_1 sin(2\theta)$$
$$-20\mathrm{i}\mu \zeta_1 sin(\theta) + (-6\lambda \zeta_2 - 66\sigma \zeta_0)]$$
$$= \zeta_0 \sum_{k=0}^{j-1} d_k^j \Phi^k (2cos(2\theta) + 52cos(\theta) + 66),$$

$$\Rightarrow 4\Phi^j[\lambda \zeta_2(sin^2(\theta) + 2sin^2(\frac{\theta}{2})) + \sigma \zeta_0(cos^2(\theta) + 26cos^2(\frac{\theta}{2}) + 3)$$
$$-\frac{\mathrm{i}\mu \zeta_1}{2}(sin(2\theta) + 10sin(\theta))]$$
$$= 4\zeta_0 \sum_{k=0}^{j-1} d_k^j \Phi^k (cos^2(\theta) + 26cos^2(\frac{\theta}{2}) + 3). \tag{37}$$

Now, from Eq. (37), one can conclude that

$$\Phi^j = \frac{\zeta_0 \eta_2 \sum_{k=0}^{j-1} d_k^j \Phi^k}{\lambda \zeta_2 \eta_1 + \sigma \zeta_0 \eta_2 - \frac{\mathrm{i}\mu \zeta_1}{2}\eta_3}$$
$$\leq \frac{\zeta_0 \eta_2 \Phi_{max}^k \sum_{k=0}^{j-1} d_k^j}{\lambda \zeta_2 \eta_1 + \sigma \zeta_0 \eta_2 - \frac{\mathrm{i}\mu \zeta_1}{2}\eta_3} \tag{38}$$
$$\leq \frac{\sigma \zeta_0 \eta_2 \Phi_{max}^{j-1}}{\lambda \zeta_2 \eta_1 + \sigma \zeta_0 \eta_2 - \frac{\mathrm{i}\mu \zeta_1}{2}\eta_3},$$

where

$$\eta_1 = sin^2(\theta) + 2sin^2(\frac{\theta}{2}),$$
$$\eta_2 = cos^2(\theta) + 26cos^2(\frac{\theta}{2}) + 3,$$
$$\eta_3 = sin(2\theta) + 10sin(\theta),$$

$$|\Phi^j|^2 = \frac{(\sigma \zeta_0|\eta_2|)^2|\Phi_{max}^{j-1}|^2}{(\lambda \zeta_2 \eta_1 + \sigma \zeta_0 \eta_2)^2 + (\frac{\mu \zeta_1}{2}\eta_3)^2}$$
$$\leq |\Phi_{max}^{j-1}|^2.$$

Since

$$(\sigma \zeta_0 |\eta_2|)^2 \le (\lambda \zeta_2 \eta_1 + \sigma \zeta_0 \eta_2)^2 + (\frac{\mu \zeta_1}{2} \eta_3)^2,$$

$|\Phi^j| \le |\Phi_{max}^{j-1}|$ for $j \ge 1$ and one can easily derive that

$$|\Phi^j| \le |\Phi^0|, \quad j \ge 1. \tag{39}$$

Finally, from (35) and (39), it can be obtained that

$$|\varepsilon^j| \le |\varepsilon^0| \quad j \ge 1. \tag{40}$$

Therefore, the proposed method is unconditionally stable. □

Statement and proof of the main convergence theorems now follow.

Theorem 4. *Let* $\hat{u}^j(x) = \sum_{k=-2}^{M+2} \hat{c}_k^j s_k(x)$ *be a unique quintic spline interpolant and* $\tilde{u}^j(x) = \sum_{k=-2}^{M+2} \tilde{c}_k^j s_k(x)$ *be the approximation function to the exact solution* $u^j(x)$ *of* (1) *at the j-th time level. Further,* $f \in C^2[0,1]$ *and* $u \in C^{10}[0,1]$, *then there exists a constant R independent of* Δ_x *such that*

$$\|\hat{u}^j(x) - \tilde{u}^j(x)\|_\infty \le R(\Delta_x)^4. \tag{41}$$

Proof. At the j-th time level, one can write

$$a_1 \hat{c}_{i-2}^j + a_2 \hat{c}_{i-1}^j + a_3 \hat{c}_i^j + a_4 \hat{c}_{i+1}^j + a_5 \hat{c}_{i+2}^j$$
$$= \zeta_0 \sum_{k=0}^{j-1} d_k^j (\hat{c}_{i-2}^k + 26 \hat{c}_{i-1}^k + 66 \hat{c}_i^k + 26 \hat{c}_{i+1}^k + \hat{c}_{i+2}^k) - \hat{f}_i^j. \tag{42}$$

Consequently, it can be shown that

$$a_1(c_{i-2}^j - \hat{c}_{i-2}^j) + a_2(c_{i-1}^j - \hat{c}_{i-1}^j) + a_3(c_i^j - \hat{c}_i^j) + a_4(c_{i+1}^j - \hat{c}_{i+1}^j)$$
$$+ a_5(c_{i+2}^j - \hat{c}_{i+2}^j)$$
$$= \zeta_0 \sum_{k=0}^{j-1} d_k^j ((c_{i-2}^k - \hat{c}_{i-2}^k) + 26(c_{i-1}^k - \hat{c}_{i-1}^k) + 66(c_i^k - \hat{c}_i^k) + 26(c_{i+1}^k - \hat{c}_i^k)$$
$$+ (c_{i+2}^k - \hat{c}_{i+2}^k)) - (f_i^j - \hat{f}_i^j), \tag{43}$$

and assuming $\hat{e}_i^j = (c_i^k - \hat{c}_i^k)$ the error equation is obtained as follows

$$a_1 \hat{e}_{i-2}^j + a_2 \hat{e}_{i-1}^j + a_3 \hat{e}_i^j + a_4 \hat{e}_{i+1}^j + a_5 \hat{e}_{i+2}^j$$
$$= \zeta_0 \sum_{k=0}^{j-1} d_k^j (\hat{e}_{i-2}^k + 26 \hat{e}_{i-1}^k + 66 \hat{e}_i^k + 26 \hat{e}_i^k + \hat{c}_{i+2}^k) - (f_i^j - \hat{f}_i^j). \tag{44}$$

For $j = 1$, due to the fact that $\hat{e}_k^0 = 0$, for $k = i-2, i-1, i, i+1, i+2$, it can be derived that

$$a_1 \hat{e}_{i-2}^1 + a_2 \hat{e}_{i-1}^1 + a_3 \hat{e}_i^1 + a_4 \hat{e}_{i+1}^1 + a_5 \hat{e}_{i+2}^1$$
$$= \zeta_0 d_0^1 (\hat{e}_{i-2}^0 + 26 \hat{e}_{i-1}^0 + 66 \hat{e}_i^0 + 26 \hat{e}_i^0 + \hat{e}_{i+2}^0) - (f_i^1 - \hat{f}_i^1) \tag{45}$$
$$= -(f_i^1 - \hat{f}_i^1).$$

Using Taylor's series expansion, the following result can be obtained for sufficiently small Δ_x:

$$
\begin{aligned}
(a_1 + a_2 + a_3 + a_4 + a_5)\hat{e}_i^1 \\
= -(f_i^1 - \hat{f}_i^1).
\end{aligned}
\tag{46}
$$

Considering the established $\sum_{l=1}^{5} a_l = \sigma$, it is permissible to write that

$$
\begin{aligned}
\sigma \hat{e}_i^1 &= -(f_i^1 - \hat{f}_i^1), \\
\Rightarrow |\hat{e}_i^1| &= |\frac{(f_i^1 - \hat{f}_i^1)}{\sigma}| \le \frac{k\Delta_x^6}{\sigma} \le k_1 \Delta_x^6.
\end{aligned}
\tag{47}
$$

By the principle of mathematical induction, it is presupposed that a corresponding relation is valid for $n \le j-1$. Now we prove that the result is true for $n = j$. By using the Taylor's series expansion, the following result can be obtained for sufficiently small Δ_x:

$$
\begin{aligned}
(a_1 + a_2 + a_3 + a_4 + a_5)\hat{e}_i^j \\
= \zeta_0 \sum_{k=0}^{j-1} d_k^j(120\hat{e}_i^k) - (f_i^j - \hat{f}_i^j) \\
\le (\hat{e}_{max}^{j-1}) \sum_{k=0}^{j-1} d_k^j - (f_i^j - \hat{f}_i^j) \\
\le (\hat{e}_{max}^{j-1})\sigma - (f_i^j - \hat{f}_i^j), \\
\Rightarrow |\hat{e}_i^j| \le |\hat{e}_{max}^{j-1}| - \frac{|f_i^j - \hat{f}_i^j|}{\sigma} \\
\le k_1 \Delta_x^4 - k_2 \Delta_x^6 \\
\le k_3 \Delta_x^4,
\end{aligned}
\tag{48}
$$

where $\hat{e}_{max}^{j-1} = max\{\hat{e}_i^0, \hat{e}_i^1, ..., \hat{e}_i^{j-1}\}$. Now, subtracting (7) from (5) it can be obtained that

$$
\begin{aligned}
\tilde{u}^j(x) - \hat{u}^j(x) &= \sum_{i=-2}^{M+2}(c_i^j - \hat{c}_i^j)s^j(x) \\
&= \sum_{i=-2}^{M+2} \hat{e}_i^j s^j(x).
\end{aligned}
\tag{49}
$$

By taking the maximum norm on both sides of (49) and then using (4) and (6), it can be derived that

$$
\begin{aligned}
\|\tilde{u}^j(x) - \hat{u}^j(x)\|_\infty &\le \hat{e}_{max}^j \sum_{i=-2}^{M+2} |s^j(x)| \\
&\le \frac{93}{60} \hat{e}_{max}^j \\
&\le R(\Delta_x)^4.
\end{aligned}
\tag{50}
$$

$\square$

Theorem 5. *Let $\hat{u}^j(x)$ be a unique quintic spline interpolant to the exact solution $u^j(x)$ of Eq. (1) at the j-th time level. Further, $f \in C^2[0,1]$ and $u \in C^{10}[0,1]$, then there exists a constant R independent of Δ_x such that*

$$\|u^j(x) - \tilde{u}^j(x)\|_\infty \leq R(\Delta_x)^4. \tag{51}$$

Proof. As a consequence of Theorem 2 for case $k = 0$, it easily can be obtained that

$$\|u^j(x) - \hat{u}^j(x)\|_\infty \leq R_1(\Delta_x)^6. \tag{52}$$

Using the triangle inequality, one can write

$$
\begin{aligned}
\|u^j(x) - \tilde{u}^j(x)\|_\infty &\leq \|u^j(x) - \hat{u}^j(x)\|_\infty + \|\hat{u}^j(x) - \tilde{u}^j(x)\|_\infty \\
&\leq R_1(\Delta_x)^6 + R_2(\Delta_x)^4 \\
&\leq R(\Delta_x)^4,
\end{aligned} \tag{53}
$$

where $R = max\{R_1, R_2\}$ is a constant independent of Δ_x. Hence, theorem is proved. $\qquad\square$

Theorem 6. *Let $u^j(x)$ and $\tilde{u}^j(x)$ be the exact solution and approximate solution of problem (1), respectively. Then, the proposed scheme (31) is convergent and the solution satisfies*

$$\|u^j(x) - \tilde{u}^j(x)\|_\infty \leq C_1(\Delta_x)^4 + C_u(\Delta_t)^{2-\alpha}, \tag{54}$$

where C_1 and C_u are positive constants.

Proof. By using Theorem 5 and Eqs. (13)-(14), one can deduce the stated result. $\qquad\square$

5 Numerical results

In this section, some numerical examples are presented to elucidate the efficacy of the proposed methodology. To validate the method's performance, numerical experiments were conducted on a computing platform featuring an ADM Sempron(tm) 140 processor, 2.70GHz, with 2.00GB of RAM, utilizing custom-developed code implemented in MATLAB 2015. Across all examples, it is presupposed that $\Delta_x = 1/M, \Delta_t = 1/N$, $M = \{8, 16, 32, 64\}$ and $N = \{8, 16, 32, 64\}$ as well as the errors are calculated by the following formula

$$E_\infty = \|u(x,1) - \tilde{u}(x,1)\|_\infty. \tag{55}$$

Suppose that $E_\infty(\Delta_x, \Delta_t) = O(\Delta_x^p + \Delta_t^q)$. If Δ_x be sufficiently small, it can be written that $E_\infty(\Delta_x, \Delta_t) = c_2(\Delta_t^q)$ and $E_\infty(\Delta_x, \frac{\Delta_t}{\kappa}) = c_2(\frac{\Delta_t^q}{\kappa})$ then $\kappa^q = \frac{E_\infty(\Delta_x, \Delta_t)}{E_\infty(\Delta_x, \frac{\Delta_t}{\kappa})}$ and $q = log_\kappa\left(\frac{E_\infty(\Delta_x, \Delta_t)}{E_\infty(\Delta_x, \frac{\Delta_t}{\kappa})}\right)$. Similarly, if Δ_t is sufficiently small, we have $p = log_\kappa\left(\frac{E_\infty(\Delta_x, \Delta_t)}{E_\infty(\frac{\Delta_x}{\kappa}, \Delta_t)}\right)$. In the rest of this section, we select $\kappa = 2$ and rename the p as space convergence order (S.C.O.) and q as the time convergence order (T.C.O.).
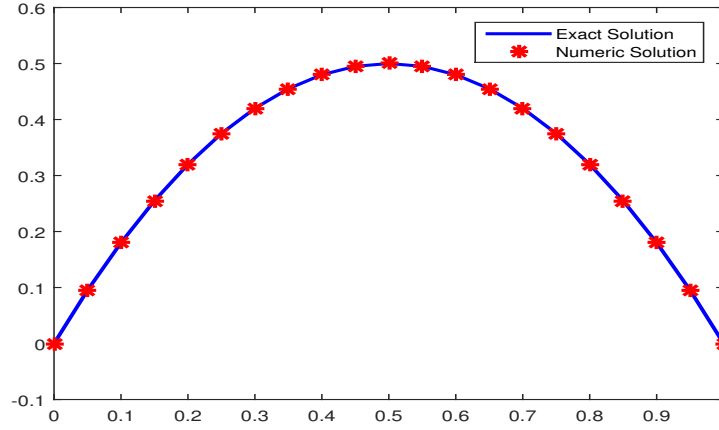
Figure 1: The exact solution and the numerical solution of the proposed method with $N = 64$, $M = 64$, $t = 1$ for Example 1

Example 1. Consider the TFADE as follows:

$$
\begin{aligned}
\partial_t^{0.5} u &= u_{xx} + \frac{6}{\Gamma(3.5)} t^{2.5} x(1-x) + 2(1+t^3), \\
u(x,0) &= x(1-x), \\
u(0,t) &= u(1,t) = 0.
\end{aligned}
\tag{56}
$$

It is clear that Eq. (56) is a heat equation, which is a special case of the advection-dispersion equation. The exact solution of this problem is $u(x,t) = x(1-x)(1+t^3)$.

The solution obtained from the proposed scheme is demonstrated in Figure 1 for $t = 1$ and Figure 2 for $0 \leq t \leq 1$.

In Table 2, the error values of Example 1 are listed for $M = 32$ and $N = 4, 8, 16, 32, 64, 128$. From this table, it can be concluded that when the time step size Δ_t is reduced by a factor of $\frac{1}{2}$, the error E_∞ decreases by about to $(\frac{1}{2})^{2-\alpha}$.

In Table 3, the error values for $M = 4, 8, 16, 32, 64$ and $N = 10000$ are shown. Considering this table, it can be derived that when the space step size Δ_x is reduced by a factor of $\frac{1}{2}$, the error E_∞ decreases by about $(\frac{1}{2})^4$. It is patently obvious that the numerical results corroborate the claims regarding the order of convergence in both time and space.

Example 2. Consider the TFADE as follows:

$$
\begin{aligned}
\partial_t^{0.5} u &= 4u_{xx} - 3u_x + \frac{6}{\Gamma(3.5)} t^{2.5} \sin(\pi x) + 4\pi^2(1+t^3)\sin(\pi x) \\
&\quad + 3\pi(1+t^3)\cos(\pi x), \\
u(0,t) &= u(1,t) = 0, \\
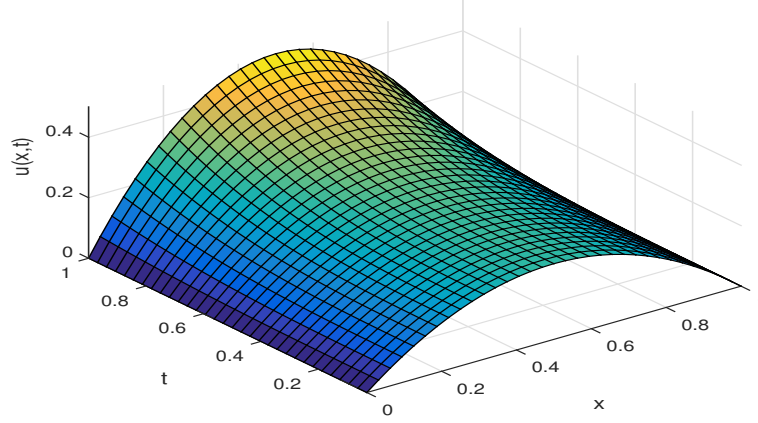u(x,0) &= \sin(\pi x).
\end{aligned}
\tag{57}
$$

Figure 2: The numerical solution by the proposed method when $N = 64, M = 64, 0 \leq t \leq 1$ for Example 1.

Table 2: Error comparison of the proposed method versus the method outlined in [12] concerning $M = 32$ and $N = 4, 8, 16, 32, 64, 128$ for Example 1

N	proposed method			method in [12]	
	E_∞	T.C.O.	C.P.U. time(s)	E_∞	T.C.O.
4	3.1311×10^{-3}	—	0.071	1.2465×10^{-2}	—
8	1.2162×10^{-3}	1.3642	0.071	3.2353×10^{-3}	1.9459
16	4.5560×10^{-4}	1.4165	0.181	8.5367×10^{-4}	1.9221
32	1.6703×10^{-4}	1.4477	0.328	2.2920×10^{-4}	1.8971
64	6.0328×10^{-5}	1.4692	0.685	6.2815×10^{-5}	1.8674
128	1.6735×10^{-5}	1.4899	1.368	1.7656×10^{-5}	1.8309

Table 3: The error values of proposed method with $M = 4, 8, 16, 32, 64, 128$ and $N = 10000$ for Example 1

	proposed method		
M	E_∞	S.C.O.	C.P.U. time(s)
4	2.9023×10^{-4}	—	412.261
8	3.3004×10^{-5}	3.1365	417.573
16	4.0264×10^{-6}	3.0351	438.529
32	3.2615×10^{-7}	3.6259	493.924
64	3.8338×10^{-8}	3.0887	615.630

The exact solution for this problem is $u(x,t) = (1 + t^3)sin(\pi x)$. The numerical solution of the proposed scheme is illustrated in Figure 3 for $t = 1$ and Figure 4 for $0 \leq t \leq 1$.

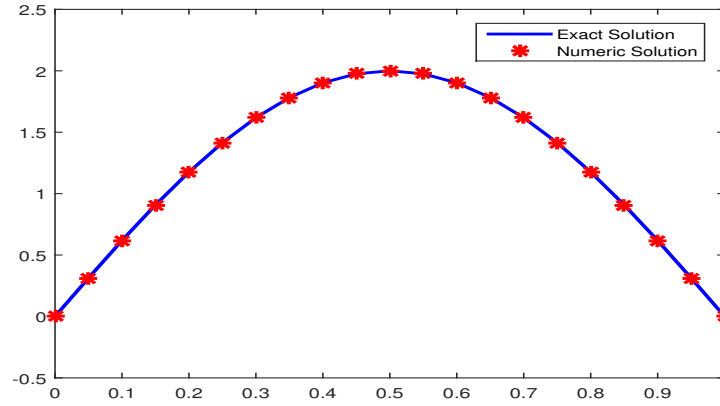In Table 4, the error values and time convergence orders are presented (for N=4,8,16,32,64,128 and

Figure 3: The exact solution and numerical solution of proposed method with $N = 64$, $M = 64$, $t = 1$ for Example 2
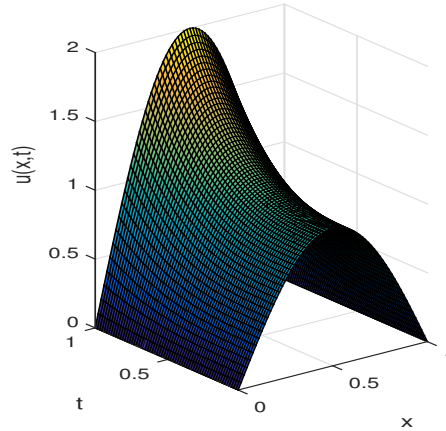

Figure 4: The numerical solution of the proposed method with $N = 64$, $M = 64$, $0 \leq t \leq 1$ for Example 2

$M = 32$) in Example 2. As evident from the table, the obtained results confirm the theoretical findings.

As evidenced by the data in Table 5 (with M=4,8,16,32,64 and $N = 10000$ for Example 2), the proposed method exhibits markedly lower errors and higher convergence rates compared to the approach in [1], demonstrating its superior computational efficacy. The improved accuracy and robust convergence behavior validate the methodological advancements of this work, setting a new standard for subsequent research in the field.

Example 3. Consider the TFADE as follows:

$$\partial_t^{0.3} u = 5u_{xx} - u_x + \frac{-60}{\Gamma(5.7)} x(x-1)t^{4.7} - 5(2 - t^5) + (2x - 1)(1 - 0.5t^5),$$

$$u(0,t) = u(1,t) = 0,$$

Table 4: The error values of proposed method with $M = 32$ and $N = 4, 8, 16, 32, 64, 128$ for Example 2

N	proposed method		
	E_∞	T.C.O.	C.P.U. time(s)
4	3.2894×10^{-3}	—	0.140
8	1.2753×10^{-3}	1.3670	0.217
16	4.7707×10^{-4}	1.4186	0.196
32	1.7466×10^{-4}	1.4496	0.360
64	6.2946×10^{-5}	1.4724	0.728
128	2.2283×10^{-5}	1.4982	1.428

Table 5: Comparison of the results of the proposed method with presented methods in [1] with N=10000 for Example 2

M	proposed method			method in [1]	
	E_∞	S.C.O.	C.P.U. time(s)	E_∞	S.C.O.
4	1.243×10^{-3}	—	423.905	1.037×10^{-1}	—
8	8.216×10^{-5}	3.9194	432.161	2.574×10^{-2}	2.0126
16	6.046×10^{-6}	3.7642	450.025	6.702×10^{-3}	1.9395
32	4.788×10^{-7}	3.6586	506.333	2.048×10^{-3}	1.7442
64	8.979×10^{-8}	2.4147	621.099	8.067×10^{-4}	1.3098

Table 6: The error values of proposed method with $M = 32$ and various values of *N* for Example 3

N	proposed method		
	E_∞	T.C.O.	C.P.U. time(s)
4	3.5390×10^{-4}	—	0.090
8	1.3592×10^{-4}	1.3806	0.112
16	4.8327×10^{-5}	1.4919	0.187
32	1.6469×10^{-5}	1.5531	0.345
64	5.4995×10^{-6}	1.5824	0.655
128	1.8424×10^{-6}	1.5777	1.333

$$u(x,0) = x(x-1).$$

The exact solution for this problem is $u(x,t) = x(x-1)(1-0.5t^5)$. Figure 5 illustrates a comparison between the numerical solution and the exact (analytical) solution for Example 3 at $t = 1$, while in Figure 6, only the numerical result obtained from the presented method is depicted in $0 \le t \le 1$. The close agreement between the two curves in Figure 5 serves as strong evidence of the high accuracy achieved by the proposed method.   Table 6 presents the error values and time convergence orders for various values of *N* and constant value $M = 32$ for example 3. The results not only corroborate theoretical predictions but also clearly demonstrate the accuracy and efficiency of the proposed method.

Table 7 encapsulates the outcomes of our proposed method, demonstrating its capability in reducing computational errors and improving accuracy. The error values systematically decrease as the underlying computational parameter *M* increases, indicating enhanced precision. Additionally, the convergence
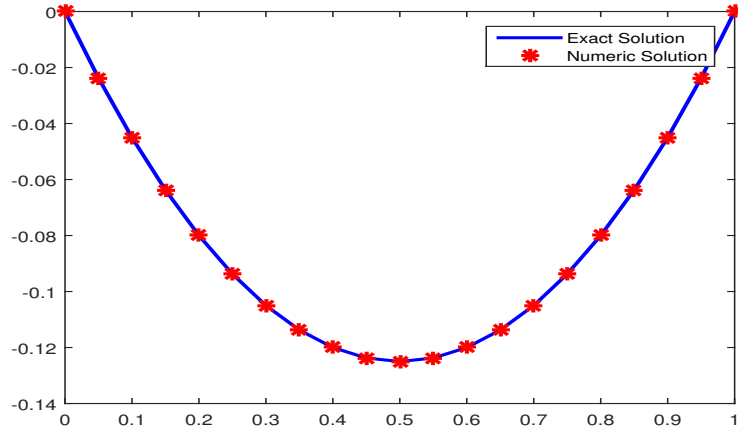
Figure 5: The comparison between the numerical solution and exact solution of Example 3 in case $N = M = 64, t = 1$
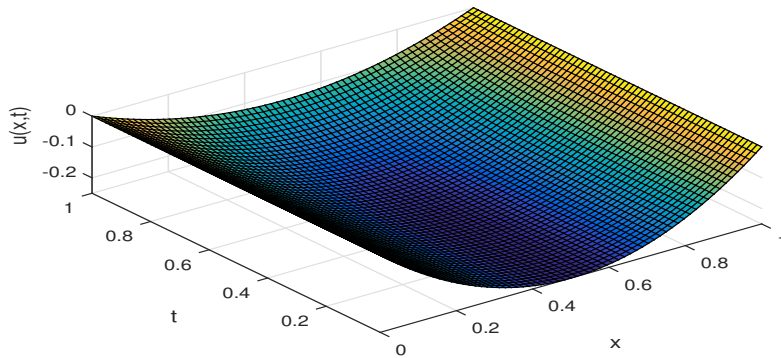

Figure 6: The numerical solution by the proposed method when $N = 64, M = 64, 0 \le t \le 1$ for Example 3

behavior showcased in the results reflects the method's efficiency in approaching the true solution with higher computational refinement.

The analysis not only highlights the method's effectiveness but also provides insights into its convergence dynamics. These findings reinforce the method's suitability for tackling complex computational challenges.

Our last example demonstrates the success of the proposed method in the case where the solution to the problem is a damped oscillatory function.

Table 7: The error values of proposed method for various values of M and $N = 10000$ by Example 3

M	proposed method		
	E_∞	S.C.O.	C.P.U. time(s)
4	7.8782×10^{-5}	—	444.394
8	9.0063×10^{-6}	3.1288	451.219
16	1.1005×10^{-6}	3.0327	476.527
32	9.2223×10^{-8}	3.5769	521.702
64	2.0281×10^{-8}	2.1850	676.036

Example 4. Consider the TFADE as follows:

$$\partial_t^\alpha u = \lambda u_{xx} - \mu u_x + f(x,t) \tag{58}$$
$$u(0,t) = u(1,t) = 0,$$
$$u(x,0) = (1+\mu)e^{-x}sin(2k\pi x),$$

where

$$f(x,t) = \left((\alpha t)^{-\alpha} E_{1,1-\alpha}(\alpha t) - \sum_{n=0}^{\lfloor \alpha \rfloor} \frac{(\alpha t)^{n-\alpha}}{\Gamma(n+1-\alpha)} \right) e^{-\lambda x} sin(2k\pi x)$$
$$- \lambda(1+\mu)e^{\alpha t - \lambda x} \left((\lambda^2 - 4k^2\pi^2)sin(2k\pi x) - 4k\pi\lambda cos(2k\pi x) \right) \tag{59}$$
$$+ \mu(1+\mu)e^{\alpha t - \lambda x} (-\lambda sin(2k\pi x) + 2k\pi cos(2k\pi x)).$$

The exact solution is

$$u(x,t) = (1+\mu)e^{\alpha t - \lambda x} sin(2k\pi x) \tag{60}$$

To get a numerical solution, put $\alpha = 0.75, \lambda = 1, \mu = 0$ and set $M = N = 64, k = 10$. The exact solution fluctuates 10 times in the interval $[0,1]$. In this case, the proposed method solve this problem in 4.392925 seconds Elapsed time. Figure 7 compares the exact solution with the approximation solution obtained from the proposed method, and Figure 8 shows its error. To get an solution with more oscillatory, put $k = 30$. In this case, the exact solution oscillatory 30 times in the interval $[0,1]$. Put $\alpha = 0.75, \lambda = 1, \mu = 0$ and $N = 256, M = 256$. In this case, the proposed method solve this problem in 63.871688 seconds Elapsed time. Figure 9 compares the exact solution with the approximation solution obtained from the proposed method, and Figure 10 shows its error.

As can be seen, when $k = 30$, the exact solution has 61 zeros in the interval $[0,1]$. To obtain an approximate solution using the spectral method, polynomials of degree at least 61 must be used, which will have a computational error. In other words, it is difficult to obtain an acceptable approximation for this problem using spectral methods. This shows the superiority of the proposed method over spectral methods.
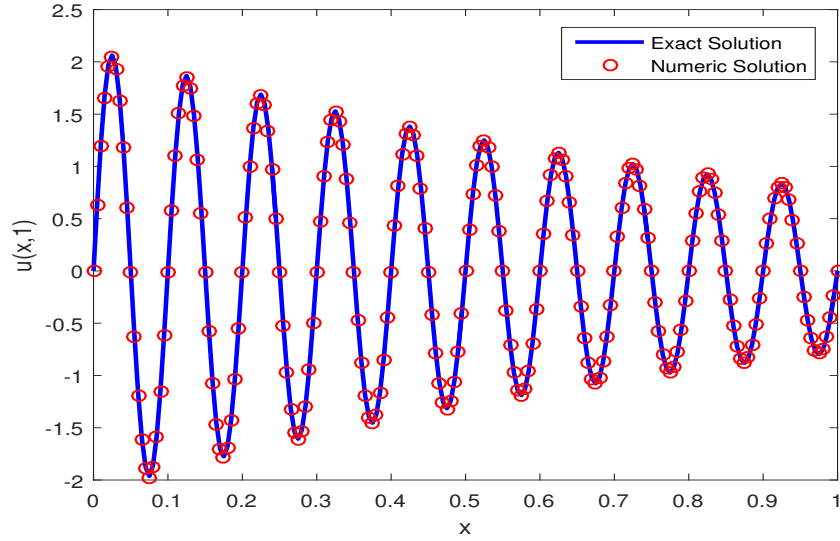
Figure 7: Comparison of the exact solution with the approximation solution obtained from the proposed method when $\alpha = 0.75, \lambda = 1, \mu = 0$ and $N = 64, M = 64, t = 1, k = 10$ for Example 4
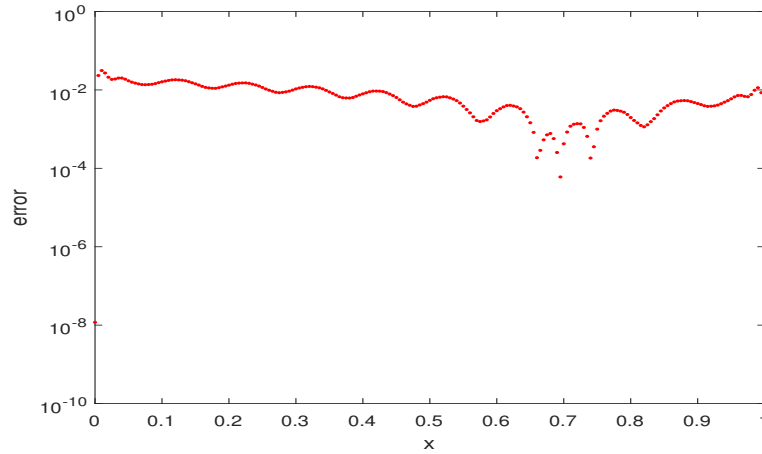

Figure 8: The error of numerical solution by the proposed method when $\alpha = 0.75$, $\lambda = 1$, $\mu = 0$ and $N = 64$, $M = 64$, $t = 1$ for Example 4

6 Conclusion

This paper presented a novel and unconditionally stable numerical method for the fractional time advection-dispersion equation. By combining the L1 scheme for temporal discretization with quintic B-spline functions for spatial approximation, the proposed approach yielded a solvable system of algebraic equations. The compelling evidence from numerical experiments unequivocally demonstrated the method's effi-
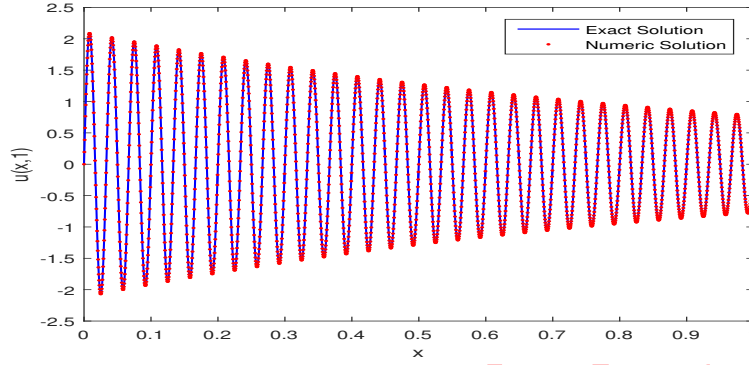
Figure 9: Comparison of the exact solution with the approximation solution obtained from the proposed method when $\alpha = 0.75$, $\lambda = 1$, $\mu = 0$ and $N = 256, M = 256, t = 1, k = 30$ for Example 4
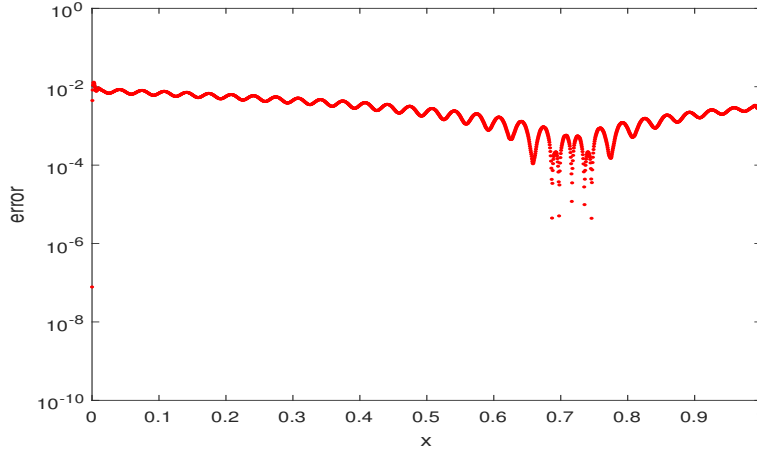

Figure 10: The error of numerical solution by the proposed method when $\alpha = 0.75$, $\lambda = 1$, $\mu = 0$ and $N = 256, M = 256, t = 1$ for Example 4

ciency and effectiveness in accurately simulating the behavior of the target equation. The development of this stable and accurate numerical tool represents a significant contribution to the field, offering a robust approach for analyzing a wide range of phenomena modeled by fractional time advection-dispersion equations. While the method performs best for smooth solutions, it handles moderately non-smooth cases (such as those with sharp gradients) more effectively than global spectral methods, due to the local support of B-splines. Extension to higher dimensions is straightforward using tensor-product B-splines, but denser matrices increase memory and computation time for large grids or 3D problems though still lower than traditional spectral methods requiring more terms or higher-degree polynomials. Efficient solvers are recommended for practical applications. Future research endeavors could explore the extension of this methodology to problems in higher spatial dimensions and investigate its applicability to nonlinear formulations of the fractional time advection-dispersion equation.

References

[1] A.H. B. Albohiwela, S. Irandoust-Pakchin, A.J. Akbarfam, *Optimal collocation method for time-fractional advection–dispersion equation using modified generalized Laguerre polynomials and particle swarm optimization algorithm*, Filomat **38(32)** (2024) 11453–11475.

[2] H. Azin, F. Mohammadi, M.H. Heydari, *A hybrid method for solving time fractional advection-diffusion equation on unbounded space domain*, Adv. Differ. Equ. **2020**(596) (2020).

[3] A. Bhardwaj, A. Kumar, *A numerical solution of time-fractional mixed diffusion and diffusion–wave equation by an RBF-based meshless method*, Eng. Comput. **38** (2022) 1883–1903.

[4] A.H. Bhrawy, *A new numerical algorithm for solving a class of fractional advection–dispersion equation with variable coefficients using Jacobi polynomials*, Abstr. Appl. Anal. (2013), Article ID 954983.

[5] S. Cao, J. Jiang, J. Wu, *Solving time-fractional advection–dispersion equation by variable weights particle tracking method*, J. Stat. Phys. **168** (2017) 1248–1258.

[6] I. Fahimi-khalilabad, S. Irandoust-pakchin, S.Abdi-mazraeh, *High-order finite difference method based on linear barycentric rational interpolation for Caputo type sub-diffusion equation*, Math. Comput. Simul. **199**, (2022), 60–80.

[7] S. Irandoust-pakchin, S. Abdi-mazraeh, A. Khani, *Numerical solution for a variable-order fractional nonlinear cable equation via Chebyshev cardinal functions*, Comput. Math. and Math. Phys. **57**, (2017), 2047–2056.

[8] S. Irandoust-pakchin, S. Abdi-mazraeh, I. Fahimi-khalilabad, *Higher order class of finite difference method for time-fractional Liouville-Caputo and space-Riesz fractional diffusion equation*, Filomat **38(2)**, (2024), 505–521.

[9] S. Irandoust-pakchin, Sh. Babapour, M Lakestani, *Image deblurring using adaptive fractional-order shock filter*, Math. Methods Appl. Sci. **44(6)**, (2021) 4907–4922.

[10] S. Irandoust-Pakchin, M. Lakestani, H. Kheiri, *Numerical approach for solving a class of nonlinear fractional differential equation*, Bull. Iran. Math. Soc., **42(5)**,(2016), 1107–1126.

[11] M. Irodotou-Ellina, E.N. Houstis, *An $O(h^6)$ quintic spline collocation method for fourth order two-point boundary value problems*, BIT **28** (1988) 288–301.

[12] I. Karatay, N. Kale, S.R. Bayramoglu, *A new difference scheme for time fractional heat equations based on the Crank–Nicolson method*, Fract. Calc. Appl. Anal., **16(4)** (2013) 892–910.

[13] M.M. Khader, N.H. Sweilam, *Approximate solutions for the fractional advection-dispersion equation using Legendre pseudo-spectral method*, Comp. Appl. Math., **33** (2014) 739—750.

[14] Z. Liu, X. Li, *A Crank–Nicolson difference scheme for the time-variable fractional mobile–immobile advection–dispersion equation*, Comput. Appl. Math., **56** (2018) 391–410.

[15] C.P. Li, F. Zeng, *Numerical Methods for Fractional Calculus*, CRC Press, Boca Raton, 2015.

[16] C.E. Mejía, A. Piedrahita, *A numerical method for a time-fractional advection–dispersion equation with a nonlinear source term*, J. Appl. Math. Comput. **61** (2019) 593–609.

[17] A.S. Moghadam, M. Arabameri, M. Barfeie, *Numerical solution of space–time variable fractional order advection–dispersion equation using radial basis functions*, J. Math. Model., **10(3)** (2022) 549–562.

[18] A. Mohebbi, M. Abbaszadeh, *Compact finite difference scheme for the solution of time-fractional advection–dispersion equation*, Numer. Algorithms **63(3)** (2013) 431–452.

[19] S. Momani, Z. Odibat, *Numerical solutions of the space–time fractional advection–dispersion equation*, Numer. Methods Partial Differ. Equ. **24(6)** (2008) 549–562.

[20] I. Podlubny, *Fractional Differential Equations: An Introduction to Fractional Derivatives, Fractional Differential Equations, to Methods of Their Solution and Some of Their Applications*, Elseier, 1998.

[21] A.S.V. Ravi Kanth, S. Deepika, *Application and analysis of spline approximation for time-fractional mobile–immobile advection–dispersion equation*, Numer. Methods Partial Differ. Equ. **34(5)** (2018) 1799–1819.

[22] P. Roul, *A high accuracy numerical method and its convergence for time-fractional Black-Scholes equation governing European options*, Appl. Numer. Math. **151**, (2020) 472–493;

[23] P. Roul, V.M.K. Prasad Goura, R. Agarwal, *A new high order numerical approach for a class of nonlinear derivative dependent singular boundary value problems*, Appl. Numer. Math. **145** (2019) 315–341.

[24] P. Roul, K. Thula, V.M.K. Prasad Goura, *An optimal sixth-order quartic B-spline collocation method for solving Bratu-type and Lane-Emden type problems*, Math. Methods Appl. Sci. **42(8)** (2019) 2613–2630.

[25] V. Saw, S. Kumar, *Fourth kind shifted chebyshev polynomials for solving space fractional order advection–dispersion equation, based on collocation method and finite difference approximation*, Int. J. Appl. Comput. Math. **4** (2018), Article 82.

[26] V. Saw, S. Kumar, *Second kind Chebyshev polynomials for solving space-fractional advection–dispersion equation using collocation method*, Iran. J. Sci. Technol. A Sci. **43** (2019) 1027–1037.

[27] M. Shakeel, I. Hussain, H. Ahmad, I. Ahmad, P. Thounthong, Y.F. Zhang, *Meshless technique for the solution of time-fractional partial differential equations having real-world applications*, J. Funct. Spaces (2020), Article ID 8898309.

[28] M.K. Singh, A. Chatterjee, *Solution of one-dimensional space- and time-fractional advection–dispersion equation by homotopy perturbation method*, Acta Geophys. **65(2)** (2017) 353–361.

[29] M.K. Singh, A. Chatterjee, V.P. Singh, *Solution of one-dimensional time-fractional advection–dispersion equation by homotopy analysis method*, J. Eng. Mech. **143(9)** (2017) 1–16.

[30] H. Singh, *Jacobi collocation method for the fractional advection–dispersion equation arising in porous media*, Numer. Methods Partial Differ. Equ. **38(3)** (2020) 636–653.

[31] K. Thula, P. Roul, *A high-order B-spline collocation method for solving nonlinear singular boundary value problems arising in engineering and applied science*, Mediterr. J. Math., **15**(176) (2018).